

# Entropy stability analysis of smoothed dissipative particle dynamics

Satori Tsuzuki<sup>a</sup>

<sup>a</sup>Research Center for Advanced Science and Technology, The University of Tokyo,  
4-6-1, Komaba, Meguro-ku, Tokyo 153-8904, Japan

arXiv:1905.06332v4 [cond-mat.stat-mech] 13 Nov 2019

## Abstract

This article presents an entropy stability analysis of smoothed dissipative particle dynamics (SDPD) to review the validity of particle discretization of entropy equations. First, we consider the simplest SDPD system: a simulation of incompressible flows using an explicit time integration scheme, assuming a quasi-static scenario with constant volume, constant number of particles, and infinitesimal time shift. Next, we derive a form of entropy from the discretized entropy equation of SDPD by integrating it with respect to time. We then examine the properties of a two-particle system for a constant temperature gradient. Interestingly, our theoretical analysis suggests that there exist eight different types of entropy stability conditions, which depend on the types of kernel functions. It is found that the Lucy kernel, poly6 kernel, and spiky kernel produce the same types of entropy stability conditions, whereas the spline kernel produces different types of entropy stability conditions. Our results contribute to a deeper understanding of particle discretization.

**Keywords:** Thermodynamics, Entropy Stability Analysis, Particle Simulations

## 1. Introduction

The smoothed dissipative particle dynamics (SDPD), which was proposed by Español (2003) [1], has attracted the attention of many physicists and engineers for over a decade. The SDPD is appropriate for simulations of mesoscale flows in which thermal fluctuations are non-negligible, and it has been acknowledged in many complex flow problems (*e.g.*, cellular blood flows [2, 3] and suspension flows including polymer molecules [4]). By introducing conservation of angular momentum, the accuracy of SDPD simulations of incompressible flows has been greatly improved [5, 6]. Thus, the SDPD exhibits great potential for solving many types of thermal flow problems that exist around us.

As described in the literature [1], the governing equations of hydrodynamics with thermodynamic consistency are

$$\frac{d\rho}{dt} = -\rho\nabla \cdot \mathbf{v}, \quad (1)$$

$$\rho \frac{d\mathbf{v}}{dt} = -\nabla P + \eta\nabla^2 \mathbf{v} + \left(\zeta + \frac{\eta}{3}\right)\nabla\nabla \cdot \mathbf{v}, \quad (2)$$

$$T\rho \frac{ds}{dt} = \phi + \kappa\nabla^2 T. \quad (3)$$

Here,  $\rho$ ,  $\kappa$ ,  $\eta$ , and  $\zeta$  are density, thermal conductivity, sheer viscosity, and bulk viscosity, respectively. The set of Eq. (1) and Eq. (2) represents the Navier–Stokes equations, and Eq. (3) represents the relationship among the entropy  $s$ , viscous heating field  $\phi$ , and temperature field  $T$ . Hereinafter, we refer to Eq. (3) as the ‘Batchelor’s equation’, as in [7].

Because the SDPD is a kind of Lagrangian particle method, each of Eq. (1) to Eq. (3) is discretized using particles in a similar manner to smoothed particle hydrodynamics (SPH) [8, 9]. According to Eq. (32) in [1], the discretized expression for the rate of change of the total entropy  $S$  is represented as

$$\frac{dS}{dt} = \sum_i \frac{\phi_i}{T_i} + \kappa \sum_{ij} \frac{F_{ij}}{d_i d_j T_i T_j} T_{ij}^2. \quad (4)$$

Here,  $T_i$  and  $T_j$  are the temperature of the  $i$ th and  $j$ th particles, respectively. The viscous heating field  $\phi_i$ , parameter  $d_i$ , relative temperature  $T_{ij}$ , and relative function  $F_{ij}$  are given as

$$\begin{aligned} \phi_i &= \left(\frac{5\eta}{6} - \frac{\zeta}{2}\right) \sum_j \frac{F_{ij}}{d_i d_j} \mathbf{v}_{ij}^2 \\ &+ \frac{5}{2} \left(\zeta + \frac{\eta}{3}\right) \sum_j \frac{F_{ij}}{d_i d_j} (\mathbf{e}_{ij} \cdot \mathbf{v}_{ij})^2, \end{aligned} \quad (5)$$

$$d_i = \sum_j W(|\mathbf{r}_{ij}|), \quad (6)$$

$$T_{ij} = T_i - T_j, \quad (7)$$

$$F_{ij} = F(|\mathbf{r}_{ij}|). \quad (8)$$

where the relative vector  $\mathbf{r}_{ij}$ , unit vector  $\mathbf{e}_{ij}$ , relative velocity  $\mathbf{v}_{ij}$ , kernel function  $W$ , and its gradient function  $F$  are given as

$$\mathbf{r}_{ij} = \mathbf{r}_i - \mathbf{r}_j, \quad (9)$$

$$\mathbf{e}_{ij} = \frac{\mathbf{r}_{ij}}{|\mathbf{r}_{ij}|}, \quad (10)$$

$$\mathbf{v}_{ij} = \mathbf{v}_i - \mathbf{v}_j, \quad (11)$$

$$W(r) = \frac{105}{16\pi h^3} \left(1 + 3\frac{r}{h}\right) \left(1 - \frac{r}{h}\right)^3, \quad (12)$$

*Email address:* tsuzuki.satori@mail.u-tokyo.ac.jp (Satori Tsuzuki)

$$\begin{aligned}
F(r) &:= \frac{1}{\mathbf{r}} \nabla W(r) \\
&= \frac{315}{4\pi h^5} \left(1 - \frac{r}{h}\right)^2.
\end{aligned} \tag{13}$$

Additionally, the parameter  $h$  ( $h > 0$ ) is the kernel radius that determines the interaction range between particles. The function  $W$  (Lucy kernel function [10]) in Eq. (12) and the function  $F$  in Eq. (13) are the reposts of Eq. (9) and Eq. (10) in [1], which presents the original SDPD.

Equation (4) represents the introduction of a weighted calculation depending on the positions of particles using the function  $F$ . Although computational physicists have discussed the validity of applying a particle discretization scheme to compute physical quantities in the case of density calculation of SPH [8, 9] or that of moving particle semi-implicit (MPS) [11, 12], the validity of applying a particle discretization scheme to the entropy calculation in Eq. (4) has not been corroborated in terms of theoretical thermodynamics, even though the mathematical derivation of Eq. (4) and its expression in the GENERIC framework [13, 14, 15] were discussed in the original research [1].

The primary purpose of this article is to discuss the thermodynamic validity of Eq. (4) in SDPD. Our strategies are as follows. First, we consider a quasi-static scenario with constant volume, constant number of particles, and infinitesimal time shift, assuming the moment of an explicit SDPD simulation of incompressible flows. Next, we derive a form of entropy from the discretized entropy equation of SDPD by integrating it with respect to time. We then examine whether the SDPD system exhibits physically reasonable behaviours by performing thermodynamic entropy analysis.

The remainder of this article is structured as follows. Section 2 derives the form of entropy from Eq. (4). In Section 3, we examine the characteristics of a two-particle system of SDPD by examining entropy stability conditions. Finally, Section 4 summarizes our results and concludes the article.

## 2. Derivation of entropy

Let us consider the case that time  $t$  varies from  $t_0$  to  $\tau$ , and temperature  $T_i$  of the  $i$ th particle ( $i = 1, 2, \dots, N$ ) varies from  $T_i^0$  to  $T_i^\tau$  in Kelvin. Let the time  $\tau$  be between  $t_0$  and  $t_0 + \Delta t$ . In this paper, we focus on the simplest SDPD system, which is an explicit simulation of incompressible flows using a forward-Euler time integration scheme [16]. Under this premise, the left-hand side of Eq. (4) is approximated by the ratio of infinitesimal entropy  $\Delta S$  to infinitesimal time  $\Delta t$  ( $dS/dt \approx \Delta S/\Delta t$ ) in the simulation space. The positions and velocities of all particles are fixed during the interval of  $\Delta t$ . Also, the values of  $d_i$ ,  $d_j$ , and  $F_{ij}$  become constant in this interval. Accordingly, the viscous heating field  $\phi_i$  of Eq. (5) becomes a constant field during  $\Delta t$ . To summarize, the time-dependant variables on the right-hand side of Eq. (4) become  $T_i$  and  $T_j$ ; hereinafter, we denote the temperature  $T_i$  as  $T_i(t)$  when we need to expressly show the time-dependency.

### 2.1. General case of $N$ particles

We derive the form of entropy  $S$  by integrating both sides of Eq. (4) over time:

$$\begin{aligned}
\int_{t_0}^{\tau} \frac{dS}{dt} dt &= \int_{t_0}^{\tau} \sum_i \frac{\phi_i}{T_i(t)} dt \\
&+ \int_{t_0}^{\tau} \kappa \sum_{ij} \frac{F_{ij}}{d_i d_j T_i(t) T_j(t)} T_{ij}(t)^2 dt.
\end{aligned} \tag{14}$$

By changing the order of integration and summation, Eq. (14) can be rewritten as

$$\begin{aligned}
\int_{t_0}^{\tau} \frac{dS}{dt} dt &= \sum_i \phi_i \int_{t_0}^{\tau} \frac{1}{T_i(t)} dt \\
&+ \kappa \sum_{ij} \frac{F_{ij}}{d_i d_j} \int_{t_0}^{\tau} \frac{T_{ij}(t)^2}{T_i(t) T_j(t)} dt.
\end{aligned} \tag{15}$$

The first term of Eq. (15) can be rewritten using the definition of definite integration by substitution [17] as

$$\begin{aligned}
\int_{t_0}^{\tau} \frac{dS}{dt} dt &= \sum_i \phi_i \int_{T_i^0}^{T_i^\tau} \frac{1}{T_i} \frac{dT_i}{dt} dt \\
&+ \kappa \sum_{ij} \frac{F_{ij}}{d_i d_j} \int_{t_0}^{\tau} \frac{T_{ij}(t)^2}{T_i(t) T_j(t)} dt, \\
\therefore \int_{t_0}^{\tau} \frac{dS}{dt} dt &= \sum_i \phi_i \int_{T_i^0}^{T_i^\tau} \frac{1}{T_i} dT_i \\
&+ \kappa \sum_{ij} \frac{F_{ij}}{d_i d_j} \int_{t_0}^{\tau} \frac{T_{ij}(t)^2}{T_i(t) T_j(t)} dt.
\end{aligned} \tag{16}$$

To integrate the second term, we introduce the concept of general topology. Let us consider the following relationship between a differentiable function  $\mathbf{G}(\mathbf{r})$  from some open subset  $U$  ( $\mathbb{R}^n$ ) to  $\mathbb{R}$  and a differentiable function  $\mathbf{r}$  from some closed interval to  $U$ . Then, by the multi-variable chain rules [18], we get

$$\mathbf{G}(\mathbf{r}) \cdot d\mathbf{r} = \mathbf{G}(\mathbf{r}(t)) \cdot \frac{d\mathbf{r}(t)}{dt} dt. \tag{17}$$

Subsequently, we can integrate both sides of Eq. (17) to get

$$\int \mathbf{G}(\mathbf{r}) \cdot d\mathbf{r} = \int \mathbf{G}(\mathbf{r}(t)) \cdot \frac{d\mathbf{r}(t)}{dt} dt. \tag{18}$$

Let us discuss the physical interpretations of the small element  $d\mathbf{r}$  and the domain of integration when we set  $\mathbf{r}$  to be  $(T_i, T_j)$ . Because we perform the integration over a small time interval, we can regard  $dT_i/dt$  and  $dT_j/dt$  as constant values in the first approximation level. Due to the symmetricity of  $i$  and  $j$  in time dependence, the relationship of  $dT_i/dt = dT_j/dt = K = \text{const}$  can be established. Hence, Eq. (18) can be expressed using the vector  $\mathbf{u} = (1, 1)$  as follows:

$$\int \mathbf{G}(\mathbf{r}(t)) \cdot \mathbf{u} dt = \frac{1}{K} \int \mathbf{G}(\mathbf{r}) \cdot d\mathbf{r}. \tag{19}$$

Meanwhile, we can choose  $\mathbf{G}(\mathbf{r})$  as

$$\mathbf{G}(\mathbf{r}(t)) = G(\mathbf{r})\mathbf{u} = \frac{T_{ij}(t)^2}{T_i(t)T_j(t)}\mathbf{u} \quad (20)$$

Although  $\mathbf{G}$  includes a singular point at  $(T_i, T_j) = (0, 0)$ , we can exclude this point from the domain of integration because temperature in Kelvin is always positive. We then obtain the following relationship:

$$\int \frac{T_{ij}(t)^2}{T_i(t)T_j(t)} dt = \frac{1}{2K} \int \mathbf{G}(\mathbf{r}) \cdot d\mathbf{r}. \quad (21)$$

Here, we use the relationship of  $\mathbf{u} \cdot \mathbf{u} = |\mathbf{u}|^2 = 2$ . In the case that we integrate the left-hand side of Eq. (21) with respect to time  $t$  in the range  $[t_0, \tau]$ , the corresponding domains of integration on the right-hand side with respect to  $T_i$  and  $T_j$  are  $[T_i^0, T_i^\tau]$  and  $[T_j^0, T_j^\tau]$ , respectively. Besides, projection of the function  $\mathbf{G}$  onto the  $T_i T_j$ -plane forms a finite area. Therefore, we regard the right-hand side as a surface integration with surface element vector  $d\mathbf{r}$  as

$$\int_{t_0}^{\tau} \frac{T_{ij}(t)^2}{T_i(t)T_j(t)} dt = \frac{1}{2K} \int_S \mathbf{G}(\mathbf{r}) \cdot d\mathbf{r}. \quad (22)$$

Here, the notation of  $S$  means that we perform the integration on the surface  $S$  on the  $T_i T_j$ -plane in the ranges  $[T_i^0, T_i^\tau]$  and  $[T_j^0, T_j^\tau]$ .

Recall that we assume forward-Euler time integration in explicit simulations. Because all the known information we can use is defined at time  $t_0$ , we use the surface element vector  $d\mathbf{r}^0$  as an alternative to  $d\mathbf{r}$ , as follows:

$$\int_{t_0}^{\tau} \frac{T_{ij}(t)^2}{T_i(t)T_j(t)} dt \approx \frac{1}{2K} \int_S \mathbf{G}(\mathbf{r}) \cdot d\mathbf{r}^0. \quad (23)$$

We then convert the right-hand side of Eq. (23) into a double integration on the  $T_i T_j$ -plane according to the formula for a surface integral of a scalar function  $G$  over a surface  $S$  [19, 20], as

$$\frac{1}{2K} \int_S \mathbf{G}(\mathbf{r}) \cdot d\mathbf{r}^0 \quad (24)$$

$$= \frac{1}{2K} \int_S G(\mathbf{r})\mathbf{u} \cdot \mathbf{u} d\mathbf{r}^0 \quad (25)$$

$$= \frac{1}{K} \int_S G(\mathbf{r}) d\mathbf{r}^0 \quad (26)$$

$$= \frac{1}{K} \int_{T_j^0}^{T_j^\tau} \int_{T_i^0}^{T_i^\tau} G(T_i, T_j) \left| \frac{\partial \mathbf{r}^0}{\partial T_i} \times \frac{\partial \mathbf{r}^0}{\partial T_j} \right| dT_i dT_j, \quad (27)$$

where

$$\left| \frac{\partial \mathbf{r}^0}{\partial T_i} \times \frac{\partial \mathbf{r}^0}{\partial T_j} \right| = \left( \frac{\partial T_i^0}{\partial T_i} \right) \left( \frac{\partial T_j^0}{\partial T_j} \right) - \left( \frac{\partial T_i^0}{\partial T_j} \right) \left( \frac{\partial T_j^0}{\partial T_i} \right). \quad (28)$$

Each element of the right-hand side in Eq. (28) represents the gradient of  $T_i$  or  $T_j$  on the  $T_i T_j$ -plane at time  $t_0$ . Similarly to the aforementioned case of their time differential, we approximate

these gradients as constant. Thus, Eq. (23) can be rewritten using Eq. (27), Eq. (28), and a constant value  $M$  as follows:

$$\begin{aligned} \int_{t_0}^{\tau} \frac{T_{ij}(t)^2}{T_i(t)T_j(t)} dt &= \frac{1}{K} \int_{T_j^0}^{T_j^\tau} \int_{T_i^0}^{T_i^\tau} G(T_i, T_j) M dT_i dT_j, \\ &= \frac{M}{K} \int_{T_j^0}^{T_j^\tau} \int_{T_i^0}^{T_i^\tau} G(T_i, T_j) dT_i dT_j, \end{aligned} \quad (29)$$

where

$$M = \left| \frac{\partial \mathbf{r}^0}{\partial T_i} \times \frac{\partial \mathbf{r}^0}{\partial T_j} \right| = \text{const}. \quad (30)$$

By substituting Eq. (7) and Eq. (29) into Eq. (16), we obtain

$$\begin{aligned} \int_{t_0}^{\tau} \frac{dS}{dt} dt &= \sum_i \phi_i \int_{T_i^0}^{T_i^\tau} \frac{1}{T_i} dT_i \\ &+ \bar{\kappa} \sum_{ij} \frac{F_{ij}}{d_i d_j} \int_{T_j^0}^{T_j^\tau} \int_{T_i^0}^{T_i^\tau} \frac{(T_i - T_j)^2}{T_i T_j} dT_i dT_j. \end{aligned} \quad (31)$$

Here,  $\bar{\kappa} = \kappa M / K$ . For simplicity, in this paper, we confine  $\bar{\kappa}$  to the case of  $\bar{\kappa} > 0$ .

By integrating the left-hand side of Eq. (31), we obtain

$$\begin{aligned} S(\tau) &= S(t_0) + \sum_i \phi_i \int_{T_i^0}^{T_i^\tau} \frac{1}{T_i} dT_i \\ &+ \bar{\kappa} \sum_{ij} \frac{F_{ij}}{d_i d_j} \int_{T_j^0}^{T_j^\tau} \int_{T_i^0}^{T_i^\tau} \frac{(T_i - T_j)^2}{T_i T_j} dT_i dT_j. \end{aligned} \quad (32)$$

Here,  $S(t_0)$  indicates the initial entropy at time  $t_0$ . Finally, by performing integration of the second term with respect to  $T_i$  and double integration of the third term on the right-hand side of Eq. (32) with respect to  $T_i$  and  $T_j$ , we obtain the form of entropy of SDPD at time  $\tau$  for the general case of  $N$  particles:

$$\begin{aligned} S(\tau) &= S(t_0) + \sum_i \phi_i \ln \left( \frac{T_i^\tau}{T_i^0} \right) + \frac{\bar{\kappa}}{2} \sum_{ij} \frac{F_{ij}}{d_i d_j} O_{ij}, \\ O_{ij} &= \left\{ (T_i^\tau)^2 - (T_i^0)^2 \right\} \ln \left( \frac{T_j^\tau}{T_j^0} \right) \\ &+ \left\{ (T_j^\tau)^2 - (T_j^0)^2 \right\} \ln \left( \frac{T_i^\tau}{T_i^0} \right) \\ &- 4 (T_i^\tau - T_i^0) (T_j^\tau - T_j^0). \end{aligned} \quad (33)$$

## 2.2. Specific case of two particles

When  $N = 2$ , Eq. (33) can be written as

$$\begin{aligned} S(\tau) &= S(t_0) + \phi_1 \ln \left( \frac{T_1^\tau}{T_1^0} \right) + \phi_2 \ln \left( \frac{T_2^\tau}{T_2^0} \right) \\ &+ \left( \frac{\bar{\kappa} F_{12}}{2d_1 d_2} + \frac{\bar{\kappa} F_{21}}{2d_2 d_1} \right) \left\{ (T_1^\tau)^2 - (T_1^0)^2 \right\} \ln \left( \frac{T_2^\tau}{T_2^0} \right) \\ &+ \left( \frac{\bar{\kappa} F_{12}}{2d_1 d_2} + \frac{\bar{\kappa} F_{21}}{2d_2 d_1} \right) \left\{ (T_2^\tau)^2 - (T_2^0)^2 \right\} \ln \left( \frac{T_1^\tau}{T_1^0} \right) \\ &- 4 \left( \frac{\bar{\kappa} F_{12}}{2d_1 d_2} + \frac{\bar{\kappa} F_{21}}{2d_2 d_1} \right) (T_1^\tau - T_1^0) (T_2^\tau - T_2^0). \end{aligned} \quad (34)$$

Because the symmetries of  $d_i$  and  $F_{ij}$  ( $i = 1, 2$ ) can be confirmed from Eq. (6) and Eq. (8) in the case of  $N = 2$ , the relationships  $d_1 = d_2$  and  $F_{12} = F_{21}$  are true. Hence, the constant parameters of  $d$ ,  $F$ , and  $\alpha$  can be introduced as

$$\alpha := \frac{\bar{k}F}{d^2}, \quad (35)$$

$$d := d_1 = d_2, \quad (36)$$

$$F := F_{12} = F_{21}. \quad (37)$$

Likewise, the viscous heating fields of  $\phi_1$  and  $\phi_2$  become equal. The parameter  $\phi$  can be introduced as

$$\begin{aligned} \phi &= \phi_1 = \phi_2, \\ \phi &= \frac{\alpha}{\bar{k}} \left( \frac{5\eta}{6} - \frac{\zeta}{2} \right) (\mathbf{v}_{ij})^2 + \frac{5\alpha}{2\bar{k}} \left( \zeta + \frac{\eta}{3} \right) (\mathbf{e}_{ij} \cdot \mathbf{v}_{ij})^2. \end{aligned} \quad (38)$$

Let us recall that the vectors of  $\mathbf{e}_{ij}$  and  $\mathbf{v}_{ij}$  become constant between  $t_0$  and  $t_0 + \Delta t$ . By using the parameters from Eq. (35) to Eq. (38), Eq. (34) can be simply rewritten as

$$\begin{aligned} S(\tau) &= S(t_0) \\ &+ \left[ \phi + \alpha \left\{ (T_1^\tau)^2 - (T_1^0)^2 \right\} \right] \ln \left( \frac{T_2^\tau}{T_2^0} \right) \\ &+ \left[ \phi + \alpha \left\{ (T_2^\tau)^2 - (T_2^0)^2 \right\} \right] \ln \left( \frac{T_1^\tau}{T_1^0} \right) \\ &- 4\alpha (T_1^\tau - T_1^0) (T_2^\tau - T_2^0). \end{aligned} \quad (39)$$

### 2.3. Characteristics of the parameter $\alpha$

As a foundation for the next section, let us examine the characteristics of the parameter  $\alpha$ . The detailed expression of Eq. (35) is written as

$$\begin{aligned} \alpha &= C_\alpha \Lambda(r), \\ C_\alpha &= \bar{k} \left( \frac{315}{4\pi h^5} \right) \left( \frac{105}{16\pi h^3} \right)^{-2} = \text{const.}, \\ \Lambda(r) &= \frac{\left(1 - \frac{r}{h}\right)^2}{\left(1 + 3\frac{r}{h}\right)^2 \left(1 - \frac{r}{h}\right)^6}. \end{aligned} \quad (40)$$

Here,  $C_\alpha > 0$  because  $\bar{k} > 0$ . Figure 1 shows the function of  $\Lambda(r)$  in Eq. (40). Here,  $\Lambda(r)$  is confirmed to become an increasing function after  $r/h > 1/9$ , and it is larger than zero within the range of  $0 \leq r/h \leq 1$ . Hence, the resulting  $\alpha$  becomes positive within  $0 \leq r/h \leq 1$ . Although the function  $\Lambda(x)$  becomes discontinuous for  $r/h \gg 1$ , the region of  $r/h \gg 1$  is not referred to in the SDPD, so this is not a problem.

In the next section, we discuss the characteristics of a two-particle system of SDPD regarding the thermodynamic validity by examining entropy stability conditions.

## 3. Entropy stability analysis

### 3.1. Derivation of entropy stability conditions

Denote the number of particles as  $N$ , the volume of the system as  $V$ , and the internal energy as  $U$ . Under the conditions

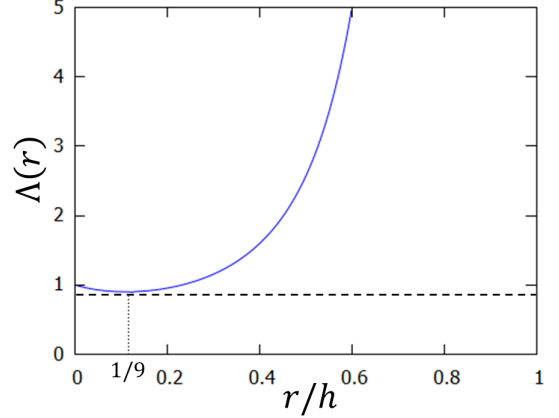


Figure 1: Function of  $\Lambda(r)$ .

of a constant volume process and fixed number of particles ( $N = V = \text{const.}$ ), an entropy stability condition is derived from a thought experiment in which two identical systems transfer an infinitesimal internal energy  $\Delta U$  between each other. If the entropy is stable, it does not increase regardless of the transfer (namely,  $S(U - \Delta U) + S(U + \Delta U) < 2S(U)$ ). By taking the Taylor series expansion of both sides of this relationship, we obtain the following stability condition [21]:

$$\left. \frac{\partial^2 S}{\partial U^2} \right|_{V,N} \leq 0. \quad (41)$$

Let us impose the condition of Eq. (41) on the entropy  $S$  in Eq. (39). The left-hand side of Eq. (41), i.e., the second-order partial derivatives of the entropy  $S$  by the internal energy  $U$ , is calculated by the following processes. First, we derive the first-order partial derivatives of  $S$  from the temperatures  $T_1^\tau$  and  $T_2^\tau$  as

$$\begin{aligned} \frac{\partial S}{\partial T_1^\tau} &= 2\alpha T_1^\tau \ln \left( \frac{T_2^\tau}{T_2^0} \right) \\ &+ \frac{\left[ \phi + \alpha \left\{ (T_2^\tau)^2 - (T_2^0)^2 \right\} \right]}{T_1^\tau} \\ &- 4\alpha (T_2^\tau - T_2^0), \end{aligned} \quad (42)$$

$$\begin{aligned} \frac{\partial S}{\partial T_2^\tau} &= 2\alpha T_2^\tau \ln \left( \frac{T_1^\tau}{T_1^0} \right) \\ &+ \frac{\left[ \phi + \alpha \left\{ (T_1^\tau)^2 - (T_1^0)^2 \right\} \right]}{T_2^\tau} \\ &- 4\alpha (T_1^\tau - T_1^0), \end{aligned} \quad (43)$$

$$\frac{\partial}{\partial T_2^\tau} \left( \frac{\partial S}{\partial T_1^\tau} \right) = 2\alpha \left( \frac{T_1^\tau}{T_2^\tau} + \frac{T_2^\tau}{T_1^\tau} - 2 \right), \quad (44)$$

$$\frac{\partial}{\partial T_1^\tau} \left( \frac{\partial S}{\partial T_2^\tau} \right) = 2\alpha \left( \frac{T_2^\tau}{T_1^\tau} + \frac{T_1^\tau}{T_2^\tau} - 2 \right), \quad (45)$$

$$\frac{\partial}{\partial T_2^\tau} \left( \frac{\partial S}{\partial T_1^\tau} \right) = \frac{\partial}{\partial T_1^\tau} \left( \frac{\partial S}{\partial T_2^\tau} \right), \quad (46)$$

$$\begin{aligned} \frac{\partial}{\partial T_1^\tau} \left( \frac{\partial S}{\partial T_1^\tau} \right) &= 2\alpha \ln \left( \frac{T_2^\tau}{T_2^0} \right) \\ &\quad - \left[ \phi + \alpha \left\{ (T_2^\tau)^2 - (T_2^0)^2 \right\} \right] \\ &\quad + \frac{\quad}{T_1^{\tau 2}}, \end{aligned} \quad (47)$$

$$\begin{aligned} \frac{\partial}{\partial T_2^\tau} \left( \frac{\partial S}{\partial T_2^\tau} \right) &= 2\alpha \ln \left( \frac{T_1^\tau}{T_1^0} \right) \\ &\quad - \left[ \phi + \alpha \left\{ (T_1^\tau)^2 - (T_1^0)^2 \right\} \right] \\ &\quad + \frac{\quad}{T_2^{\tau 2}}. \end{aligned} \quad (48)$$

The heat capacity  $C_V$  under an isochoric process is given by

$$\left. \frac{\partial T_i^\tau}{\partial U} \right|_V = \left. \frac{dT_i^\tau}{dU} \right|_{dV=0} = \frac{1}{C_V} = \text{const.} \quad (i = 1, 2). \quad (49)$$

Meanwhile, the left-hand side of Eq. (41) can be rewritten as follows [21]:

$$\begin{aligned} \left. \frac{\partial^2 S}{\partial U^2} \right|_{V,N} &= \left( \frac{\partial^2 S}{\partial T_1^{\tau 2}} \right) \left( \frac{dT_1^\tau}{dU} \right)^2 \\ &\quad + 2 \frac{\partial}{\partial T_1^\tau} \left( \frac{\partial S}{\partial T_2^\tau} \right) \left( \frac{dT_1^\tau}{dU} \right) \left( \frac{dT_2^\tau}{dU} \right) \\ &\quad + \left( \frac{\partial^2 S}{\partial T_2^{\tau 2}} \right) \left( \frac{dT_2^\tau}{dU} \right)^2 \\ &\quad + \left( \frac{\partial S}{\partial T_1^\tau} \right) \left( \frac{d^2 T_1^\tau}{dU^2} \right) + \left( \frac{\partial S}{\partial T_2^\tau} \right) \left( \frac{d^2 T_2^\tau}{dU^2} \right). \end{aligned} \quad (50)$$

Here, the fourth and fifth terms vanish because of Eq. (49). Using Eq. (42) to Eq. (50), we obtain the following entropy stability condition:

$$\begin{aligned} \frac{1}{C_V^2} &\left[ \frac{-\left\{ \phi + \alpha \left( (T_2^\tau)^2 - (T_2^0)^2 \right) \right\}}{T_1^{\tau 2}} \right. \\ &\quad \left. - \frac{-\left\{ \phi + \alpha \left( (T_1^\tau)^2 - (T_1^0)^2 \right) \right\}}{T_2^{\tau 2}} \right] \\ &+ 4\alpha \left\{ \frac{1}{2} \ln \left( \frac{T_1^\tau}{T_1^0} \right) + \frac{1}{2} \ln \left( \frac{T_2^\tau}{T_2^0} \right) + \frac{T_2^\tau}{T_1^\tau} + \frac{T_1^\tau}{T_2^\tau} - 2 \right\} \leq 0, \end{aligned} \quad (51)$$

$$\begin{aligned} \therefore &\frac{\phi + \alpha \left( (T_2^\tau)^2 - (T_2^0)^2 \right)}{T_1^{\tau 2}} \\ &+ \frac{\phi + \alpha \left( (T_1^\tau)^2 - (T_1^0)^2 \right)}{T_2^{\tau 2}} \\ &- 4\alpha \left\{ \frac{1}{2} \ln \left( \frac{T_1^\tau}{T_1^0} \right) + \frac{1}{2} \ln \left( \frac{T_2^\tau}{T_2^0} \right) + \frac{T_2^\tau}{T_1^\tau} + \frac{T_1^\tau}{T_2^\tau} - 2 \right\} \geq 0. \end{aligned} \quad (52)$$

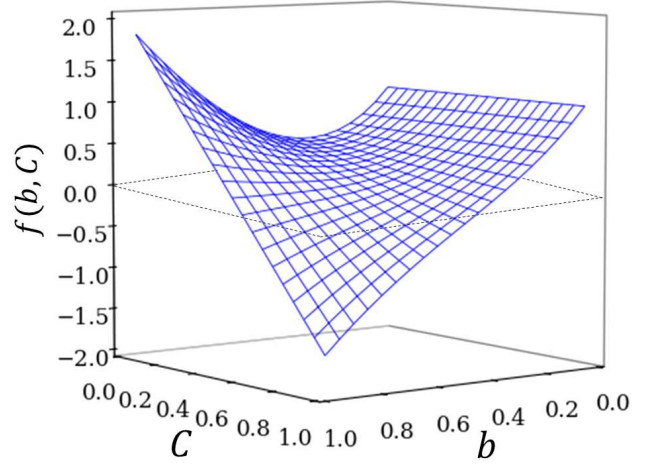


Figure 2: Fourth-order function of  $f(b, C)$  described by Eq. (55).

### 3.2. Theoretical analyses with case studies

To reproduce a system with a constant temperature gradient, we impose a constraint on the domain of integration as follows:

$$T_2^\tau = bT_1^\tau, \quad T_2^0 = bT_1^0, \quad b > 0. \quad (53)$$

Equation (53) suggests that a linear temperature relationship is imposed before and after the time evolution. By substituting the right-hand side of the two equations in Eq. (53) into Eq. (52), we obtain

$$\alpha f(b, C) T_1^\tau \geq \alpha (b^4 + 1) T_1^0 - \phi (b^2 + 1), \quad (54)$$

where

$$\begin{aligned} f(b, C) &= b^4 - 4b^3 \\ &\quad + (8 - 4C)b^2 - 4b + 1, \\ C &:= \ln \left( \frac{T_1^\tau}{T_1^0} \right). \end{aligned} \quad (55)$$

Because  $\alpha > 0$ , the sign of the left-hand side of Eq.(54) is determined by the sign of the function  $f(b, C)$ . Figure 2 shows a contour plot of  $f(b, C)$ . The function  $f(b, C)$  increases as the parameter  $b$  increases when  $C = 0$ , whereas it decreases as  $b$  increases when  $C \gg 0$ . It is confirmed that there exist critical values  $C_c$  where  $f(b, C) = 0$ . Therefore, the stability condition is distinguished by the function  $f(b, C)$  as

$$\begin{cases} f(b, C) \geq 0 & T_1^\tau \geq \frac{\alpha(b^4+1)T_1^0 - \phi(b^2+1)}{\alpha f(b,C)}, \\ f(b, C) \leq 0 & T_1^\tau \leq \frac{\alpha(b^4+1)T_1^0 - \phi(b^2+1)}{\alpha f(b,C)}. \end{cases} \quad (56)$$

In the case that the parameter  $b$  is sufficiently close to 1 (i.e., the temperature gradient between two particles is moderate), Eq. (56) works as a stabilizer of the system; it gives the maximum temperature limit as  $T_1^\tau$  increases and reaches the high-temperature area where  $f(b, C) \leq 0$ , whereas it gives the minimum temperature limit as  $T_1^\tau$  decreases and reaches the low-temperature area where  $f(b, C) \geq 0$ . Meanwhile, when the parameter  $b$  is sufficiently close to 0 (i.e., the temperature gradient

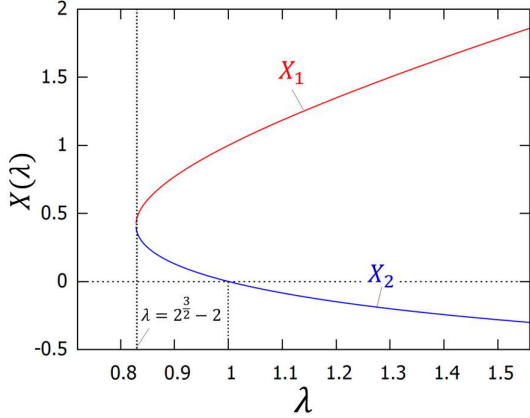


Figure 3: Dependencies of  $X_1$  and  $X_2$  on the parameter  $\lambda$ .

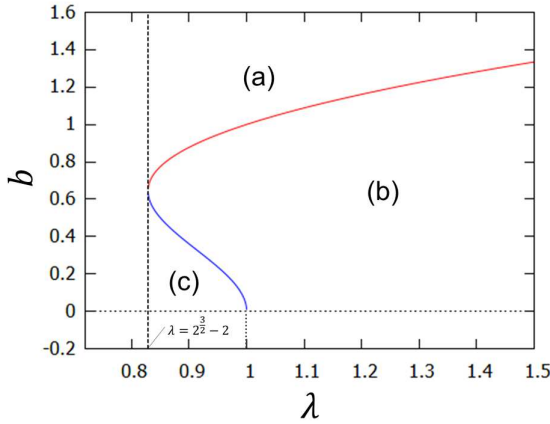


Figure 4: Classification of the state of the SDPD system determined by the parameters  $b$  and  $\lambda$  when  $f(b, C) \geq 0$ .

between two particles is steep),  $f(b, C)$  becomes positive everywhere, and the upper part of Eq. (56) is therefore required as the stability condition.

To deepen the discussion on this issue, we provide a visual representation of the case of  $f(b, C) \geq 0$  in Eq. (56). Denote the numerator of the fraction in Eq. (56) as  $D$ . Let us examine the conditions that the parameter  $D$  becomes positive as

$$D = \alpha(b^4 + 1)T_1^0 - \phi(b^2 + 1) \geq 0. \quad (57)$$

By replacing  $b^2$  with the parameter  $X$ , we obtain

$$\alpha(X^2 + 1)T_1^0 - \phi(X + 1) \geq 0, \quad X = b^2. \quad (58)$$

When the equality holds, we obtain the solutions of  $X_1$  and  $X_2$  as

$$\begin{aligned} X_1 &= \frac{\lambda + \sqrt{\lambda^2 + 4\lambda - 4}}{2}, \\ X_2 &= \frac{\lambda - \sqrt{\lambda^2 + 4\lambda - 4}}{2}, \\ \lambda &= \frac{\phi}{\alpha T_1^0}. \end{aligned} \quad (59)$$

Figure 3 shows the dependencies of  $X_1$  and  $X_2$  on the parameter  $\lambda$ . The solution of  $X_1$  is valid when  $\lambda \geq 2^{\frac{3}{2}} - 2$  and is confirmed

to satisfy  $X_1 > X_2$  everywhere. Meanwhile, the solution of  $X_2$  is valid only when  $2^{\frac{3}{2}} - 2 \leq \lambda \leq 1$ . Hence, by substituting the expressions in Eq. (59) into Eq. (58), we obtain the following conditions:

$$\begin{aligned} b &\geq \sqrt{\frac{\lambda + \sqrt{\lambda^2 + 4\lambda - 4}}{2}}, \quad \lambda \geq \lambda_0, \\ b &\leq \sqrt{\frac{\lambda - \sqrt{\lambda^2 + 4\lambda - 4}}{2}}, \quad b > 0, \quad \lambda_0 \leq \lambda \leq 1, \\ \lambda_0 &:= 2^{\frac{3}{2}} - 2. \end{aligned} \quad (60)$$

Figure 4 shows the classification of the state of the SDPD system determined by the parameters  $b$  and  $\lambda$ . In area (b), the sign of the parameter  $D$  becomes negative. In contrast, in areas (a) and (c), the sign of  $D$  becomes positive. From the results in Fig. 3 and Fig. 4 it is important to note that the sign of the parameter  $D$  could become positive or negative.

Given that the signs of  $\alpha$  and the function  $F$  are the same, we can subdivide the entropy stability conditions into eight different types, as listed in Table 1. In Type 2 and Type 8, the system becomes stable because the temperature in Kelvin must be positive, while the sign of  $D/\alpha f(b, C)$  is negative. However, in Type 3 and Type 5, the entropy becomes unstable everywhere, and no scenario satisfies the condition that the temperature becomes less than or equal to  $D/\alpha f(b, C)$  because it is negative.

The main point to emphasize from Table 1 is that the entropy stability condition of the system depends on the function  $F$ , which indicates that the types of kernel functions influence the entropy stability condition of the system. In the classical SDPD model, because it uses the Lucy kernel, the sign of the function  $F$  becomes positive. Hence, the possible types are Type 1, Type 2, Type 5, and Type 6.

Let us consider some cases using other kernel functions. In the case that we use the spiky kernel [22] or poly6 kernel [23], each  $F$  is positive everywhere in the range of  $0 < r/h < 1$ . Therefore, the possible types of entropy conditions are the same as those for the Lucy kernel. On the contrary, when we use Mao and Yang's spline kernel [24, 25, 26], the possible types of entropy conditions are Type 3, Type 4, Type 7, and Type 8 because the function  $F$  becomes negative in the range of  $0 < r/h < 1$ . For reference, Fig. 5 shows the function  $F$  in different types of kernel functions.

The fact that the kernel function contributes to the entropy stability conditions of a two-particle system can be extended to many-particle systems based on the concept of pair-wise particle methods [27, 28, 29, 30]. In these methods, the total force  $\mathbf{f}$  acted on a particle is broken down as  $\mathbf{f} = \sum \mathbf{f}_{ij}$ , where  $\mathbf{f}_{ij}$  is the force between the  $i$ th and  $j$ th particles [27]. Namely, the dynamics of a total system can be described as superpositions of two-particle modes.

Consider a case that two persons carry out simulations using the same computational conditions except for their kernel functions. If one uses the spiky kernel and the other uses the spline kernel, the entropy stability conditions imposed on an identical pair of particles differ. In this case, it could happen that only

Types	$f(b, C)$	$F$	$D$	Entropy-stability Conditions
1	+	+	+	$T_1^\tau \geq \frac{D}{\alpha f(b, C)}$
2	+	+	-	$T_1^\tau > 0$
3	+	-	+	(unstable)
4	+	-	-	$T_1^\tau \leq \frac{D}{\alpha f(b, C)}$
5	-	+	+	(unstable)
6	-	+	-	$T_1^\tau \leq \frac{D}{\alpha f(b, C)}$
7	-	-	+	$T_1^\tau \geq \frac{D}{\alpha f(b, C)}$
8	-	-	-	$T_1^\tau > 0$

Table 1: Eight different types of entropy-stability conditions depending on function  $f(b, C)$ , the parameter  $D$ , and the function  $F$ .

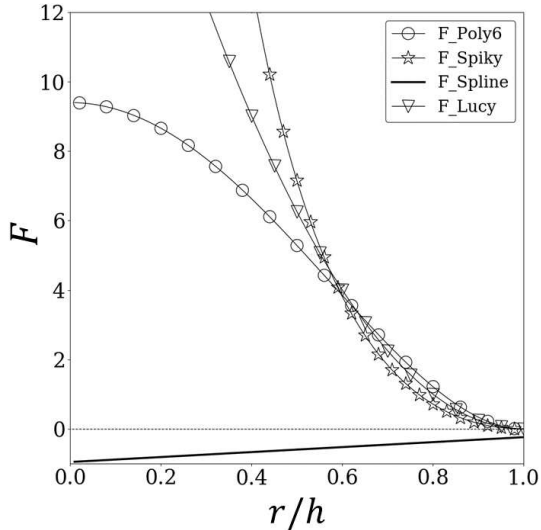


Figure 5: Comparison of function  $F$  in different types of kernel functions.

one of the systems is judged to be unstable despite them considering the same physical scenario, which could lead to the emergence of different physical phenomena, such as turbulence or heat transfer. Consequently, the dynamics of the entire multi-particle system could change. How the difference between the judges of entropy stability conditions affects the system must be investigated in future studies.

#### 4. Conclusion

In this article, we performed an entropy stability analysis of SDPD to evaluate the particle discretization of entropy equations exhibited in SDPD. First, we focused on the simplest SDPD system: a simulation of incompressible flows using an explicit time integration scheme, assuming a quasi-static scenario with constant volume, constant number of particles, and

infinitesimal time shift. Next, we derived a form of entropy from the discretized entropy equation of SDPD by integrating with respect to time. Then, we examined the properties of a two-particle system for a constant temperature gradient.

Our theoretical analysis suggests that there exist eight different types of entropy stability conditions, which depend on the types of kernel functions. It was found that the Lucy kernel, poly6 kernel, and spiky kernel produce the same types of entropy stability conditions, whereas the spline kernel produces different types of entropy stability conditions. To summarize, our results suggest that computational parameters of kernel functions contribute to the physical conditions of particle discretization systems.

It is meaningful that we theoretically analyse the two-particle system because such a system with a small number of particles cannot be simulated owing to the lack of numerical accuracy. In that sense, our analysis in this study can be regarded as a ‘thought experiment’. Our results contribute to a deeper understanding of particle discretization.

#### Acknowledgement

This research was supported by MEXT as part of the Post-K Computer Exploratory Challenges (Exploratory Challenge 2: Construction of Models for Interaction Among Multiple Socioeconomic Phenomena, Model Development and its Applications for Enabling Robust and Optimized Social Transportation Systems; Project ID: hp190163), and partially supported by JSPS KAKENHI Grant Numbers 25287026, 15K17583, and 18H06459. I would also like to express my gratitude to my family for their moral support and warm encouragement.

#### Appendix A. Further analysis on a particular point of the two-particle case in the SDPD system using the Lucy kernel

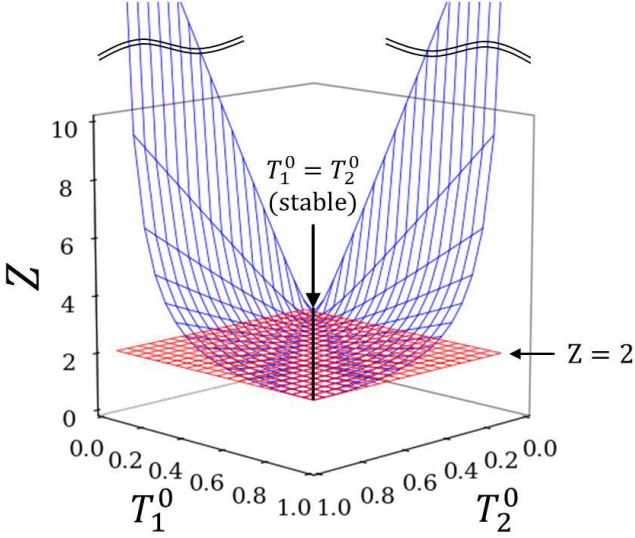


Figure A.6: Stability condition of entropy  $S$  at the initial time  $t = t_0$ .

Here, we introduce a case where the coefficients of the second and third terms of Eq. (39) become zero:

$$\phi + \alpha \left\{ (T_2^\tau)^2 - (T_2^0)^2 \right\} = 0, \quad (\text{A.1})$$

$$\phi + \alpha \left\{ (T_1^\tau)^2 - (T_1^0)^2 \right\} = 0. \quad (\text{A.2})$$

Equation (A.1) and Eq. (A.2) directly lead to

$$T_1^\tau = \sqrt{(T_1^0)^2 - \frac{\phi}{\alpha}}, \quad (\text{A.3})$$

$$T_2^\tau = \sqrt{(T_2^0)^2 - \frac{\phi}{\alpha}}. \quad (\text{A.4})$$

In this case, we can rewrite Eq. (39) as

$$S(\tau) = S(t_0) - 4\alpha\beta\gamma, \quad (\text{A.5})$$

$$\alpha := \frac{\bar{k}F}{d^2}, \quad (\text{A.6})$$

$$\beta := \sqrt{(T_1^0)^2 - \frac{\phi}{\alpha}} - T_1^0, \quad (\text{A.7})$$

$$\gamma := \sqrt{(T_2^0)^2 - \frac{\phi}{\alpha}} - T_2^0. \quad (\text{A.8})$$

Note that Eq. (A.6) is a duplicate of Eq. (35). From Eq. (A.5) and the positiveness of entropy in Kelvin, we obtain the following relationship:

$$S(\tau) = S(t_0) - 4\alpha\beta\gamma \geq 0, \quad (\text{A.9})$$

$$\therefore S(t_0) \geq 4\alpha\beta\gamma. \quad (\text{A.10})$$

The right-hand side of Eq. (A.10) indicates the minimum entropy at the initial time  $t_0$ .

Here, the state of the system can be distinguished by the constant viscous heating field  $\phi$  as follows:

- When  $\phi \neq 0$ , the relationships  $\beta\gamma > 0$  and  $\alpha > 0$  are true. Hence, the

entropy of  $4\alpha\beta\gamma$  on the right-hand side of Eq. (A.10) is always positive. There exists  $\delta (> 0)$  such that the following relationship is satisfied for all cases of  $(\alpha, \beta, \gamma)$ :

$$\exists \delta > 0, \quad 4\alpha\beta\gamma > \delta. \quad (\text{A.11})$$

Because the parameter  $\alpha$  is a function of the relative position  $r$  and the parameter  $\beta\gamma$  is a function of the temperature  $T$ ,  $\alpha$  in Eq. (A.11) can be replaced with the function  $f(r)$  and  $\beta\gamma$  with the function  $g(T)$  as

$$\exists \delta > 0, \quad f(r)g(T) > \frac{\delta}{4}. \quad (\text{A.12})$$

- When  $\phi = 0$ , the relationship of  $\beta = \gamma = 0$  is true. Hence, the value of  $4\alpha\beta\gamma$  on the right-hand side of Eq. (A.10) becomes zero. Then,

$$\phi = 0 \implies S(\tau) = S(t_0). \quad (\text{A.13})$$

The entropy stability condition can be simplified for  $\phi = 0$  as follows: Because the relationship  $T_i^\tau = T_i^0$  ( $i = 1, 2$ ) is true, the first term, second term, and logarithm functions on the left-hand side of Eq. (52) vanish. Because  $\alpha > 0$ , we obtain the stability condition as

$$\left( \frac{T_2^0}{T_1^0} + \frac{T_1^0}{T_2^0} \right) \leq 2. \quad (\text{A.14})$$

Equation (A.14) is the stability condition of the entropy  $S$  at time  $t_0$ . Figure A.6 shows the plane  $Z = 2$ , and the contour plot of the function  $Z(T_1^0, T_2^0)$  on the left-hand side of Eq. (A.14). It is confirmed that the initial state at time  $t_0$  is stable only when  $T_1^0 = T_2^0$ , at which point the temperature gradient becomes zero; this is consistent with fundamental statistical thermodynamics.

## References

- [1] P. Español and M. Revenga, Smoothed dissipative particle dynamics, *Phys. Rev. E* **67**, 026705 (2003).
- [2] D. Alizadehrad and D. A. Fedosov, Static and dynamic properties of smoothed dissipative particle dynamics, *Journal of Computational Physics* **356**, 303 (2018).
- [3] T. Ye, N. Phan-Thien, C. T. Lim, L. Peng, and H. Shi, Hybrid smoothed dissipative particle dynamics and immersed boundary method for simulation of red blood cells in flows, *Phys. Rev. E* **95**, 063314 (2017).
- [4] S. Litvinov, M. Ellero, X. Hu, and N. A. Adams, Smoothed dissipative particle dynamics model for polymer molecules in suspension, *Phys. Rev. E* **77**, 066703 (2008).
- [5] X. Y. Hu and N. A. Adams, Angular-momentum conservative smoothed particle dynamics for incompressible viscous flows, *Physics of Fluids* **18**, 101702 (2006).
- [6] K. Müller, D. A. Fedosov, and G. Gompper, Smoothed dissipative particle dynamics with angular momentum conservation, *Journal of Computational Physics* **281**, 301 (2015).
- [7] C. K. Batchelor and G. Batchelor, *An introduction to fluid dynamics* (Cambridge university press, 1967).
- [8] R. A. Gingold and J. J. Monaghan, Smoothed particle hydrodynamics: theory and application to non-spherical stars, *Monthly notices of the royal astronomical society* **181**, 375 (1977).



- [9] J. P. Morris, P. J. Fox, and Y. Zhu, Modeling low reynolds number incompressible flows using sph, *Journal of computational physics* **136**, 214 (1997).
- [10] L. B. Lucy, A numerical approach to the testing of the fission hypothesis, *The astronomical journal* **82**, 1013 (1977).
- [11] S. Koshizuka and Y. Oka, Moving-particle semi-implicit method for fragmentation of incompressible fluid, *Nuclear science and engineering* **123**, 421 (1996).
- [12] S. Koshizuka, K. Shibata, M. Kondo, and T. Matsunaga, *Moving Particle Semi-implicit Method: A Meshfree Particle Method for Fluid Dynamics* (Academic Press, 2018).
- [13] M. Grmela and H. C. Öttinger, Dynamics and thermodynamics of complex fluids. i. development of a general formalism, *Phys. Rev. E* **56**, 6620 (1997).
- [14] H. C. Öttinger and M. Grmela, Dynamics and thermodynamics of complex fluids. ii. illustrations of a general formalism, *Phys. Rev. E* **56**, 6633 (1997).
- [15] H. C. Öttinger, General projection operator formalism for the dynamics and thermodynamics of complex fluids, *Phys. Rev. E* **57**, 1416 (1998).
- [16] R. M. Corless and N. Fillion, A graduate introduction to numerical methods, *AMC* **10**, 12 (2013).
- [17] T. M. Apostol, *Mathematical analysis* (Addison-Wesley Reading, 1964).
- [18] R. E. Williamson and H. F. Trotter, Multivariable mathematics: Linear algebra, calculus, *Differential Equations* **2**.
- [19] M. Hazewinkel, Surface integral. *encyclopedia of mathematics*, 2001.
- [20] J. G. Leathem *Volume and surface integrals used in physics* No. 1 (University Press, 1922).
- [21] H. B. Callen, *Thermodynamics and an introduction to thermostatistics; 2nd ed.* (Wiley, New York, NY, 1985).
- [22] M. Desbrun and M.-P. Gascuel, Smoothed particles: A new paradigm for animating highly deformable bodies, in *Computer Animation and Simulation96*, pp. 61–76, Springer, 1996.
- [23] M. Müller, D. Charypar, and M. Gross, Particle-based fluid simulation for interactive applications, in *Proceedings of the 2003 ACM SIGGRAPH/Eurographics symposium on Computer animation*, pp. 154–159, Eurographics Association, 2003.
- [24] H. Mao and Y.-H. Yang, Particle-based non-newtonian fluid animation with heating effects, University of Alberta, Tech. Rep (2006).
- [25] J. J. Monaghan, Smoothed particle hydrodynamics, *Annual review of astronomy and astrophysics* **30**, 543 (1992).
- [26] M. Becker and M. Teschner, Weakly compressible sph for free surface flows, in *Proceedings of the 2007 ACM SIGGRAPH/Eurographics symposium on Computer animation*, pp. 209–217, Eurographics Association, 2007.
- [27] T. Yang, R. R. Martin, M. C. Lin, J. Chang, and S.-M. Hu, Pairwise force sph model for real-time multi-interaction applications, *IEEE transactions on visualization and computer graphics* **23**, 2235 (2017).
- [28] A. Tartakovsky and P. Meakin, Modeling of surface tension and contact angles with smoothed particle hydrodynamics, *Physical Review E* **72**, 026301 (2005).
- [29] U. Bandara *et al.*, Smoothed particle hydrodynamics pore-scale simulations of unstable immiscible flow in porous media, *Advances in water resources* **62**, 356 (2013).
- [30] A. M. Tartakovsky *et al.*, Smoothed particle hydrodynamics and its applications for multiphase flow and reactive transport in porous media, *Computational Geosciences* **20**, 807 (2016).